MICROCOPY RESOLUTION TEST CHART
NATIONAL BUREAU OF STANDARDS-1963-A

AD-A189 510

HOLOGRAPHICALLY CORRECTING SYNTHETIC

APERTURE ABERRATIONS

THESIS

David M. Tripp
Captain, USAF

AFIT/GEO/ENP/87D-5

DEPARTMENT OF THE AIR FORCE
AIR UNIVERSITY

AIR FORCE INSTITUTE OF TECHNOLOGY

Wright-Patterson Air Force Base, Ohio

88 3 01 175

HOLOGRAPHICALLY CORRECTING SYNTHETIC

APERTURE ABERRATIONS

THESIS

David M. Tripp
Captain, USAF

AFIT/GEO/ENP/87D-5

DTIC
ELECTE
MAR 0 2 1988
S H

AFIT/GEO/ENP/87D-5

HOLOGRAPHICALLY CORRECTING SYNTHETIC

APERTURE ABERRATIONS

THESIS

Presented to the Faculty of the School of Engineering

of the Air Force Institute of Technology

Air University

In Partial Fulfillment of the

Requirements for the Degree of

Master of Science in Electrical Engineering

David M. Tripp, B.S.

Captain, USAF

December 1987

Approved for public release; distribution unlimited

Preface

One mission of the Strategic Defense Initiative is the discrimination of targets and decoys in a space environment. The resolution needed for such a task can be provided by a synthetic aperture. The aberrations generated by the inherent misalignment of the synthetic aperture's individual optical elements must be corrected in real time before a synthetic aperture optical space system can be deployed.

Electro-optic crystals provide a means of implementing real time holographic aberration correction. Through the modulation of the crystal's refractive index by an incident optical field, a hologram can be recorded and read out within fractions of a second. The use of electro-optic crystals for real time filtering of synthetic aperture aberrations is of special interest to the Air Force and deserves further research.

I would like to thank my thesis advisor, Lt Col James P. Mills, for his guidance and support. In addition, I wish to thank Ron Gabriel for his indispensible advice in the assembly of the experimental optical systems. Finally, I want to sincerely thank my wife, Leslie, for her love, patience and understanding.

- David M. Tripp

ii

Table of Contents

List of Figures

List of Tables

AFIT/GEO/ENP/87D-5

Abstract

The effectiveness of using a bismuth silicon oxide
(BSO) electro-optic crystal to holographically correct
synthetic-aperture aberrations is investigated.   A
theoretical analysis of hologram formation in electro-optic
crystals was performed.   Experiments were then conducted
to determine the diffraction efficiency and hologram
erasure rate characteristics of the BSO crystal.   The BSO
crystal successfully performed real time aberration
correction of a single-lens optical system; but due to the
experimental synthetic-aperture optical system design, it
was impossible for the crystal to correct the synthetic-
aperture aberrations.

I.   Introduction

Problem and Scope

The problem of correcting synthetic-aperture aberrations must be solved in order for synthetic apertures to be effective. The objective of this thesis effort is to correct synthetic-aperture aberrations through the use of holograms formed in photorefractive crystals. The thesis effort includes a theoretical analysis of hologram formation in photorefractive crystals followed by a series of experiments to determine the effectiveness of using these crystals to correct synthetic-aperture aberrations.

Background

One of the most pressing problems facing the Strategic Defense Initiative (SDI) is the discrimination between targets and decoys in a space environment. The minimum resolvable angular separation between two objects when imaged through a single aperture is given by the Raleigh criteria:

$$\Delta\phi_{min} = 1.22\,\lambda/d \qquad\qquad (1)$$

where λ is the wavelength and d is the diameter of the optical element (14:354). Since the response of devices

used for detection of objects in space is usually limited
to certain wavelength bands, the only other way to achieve
greater resolution is by increasing the size of the optics.
For SDI applications, this implies that very large diameter
optical elements (>5m) are needed. Optical elements of
this size are extremely difficult and costly to fabricate;
and once obtained, there exists an even greater problem of
how to get them into space. An optic of this size exceeds
the available cargo space in the shuttle. Therefore,
another method to achieve the discussed resolution must be
used.

A promising method of obtaining greater resolution
from smaller optics is through synthetic apertures. A
synthetic aperture is realized by using one or more smaller
optical elements to achieve the resolution of a single,
large optic (11:26). The synthetic aperture shown in
Figure 1 is a representation of how smaller optical
elements can be assembled to obtain the resolution of a
larger optic.

There are, however, problems associated with using
synthetic apertures. The synthetic aperture can not
collect as much light as a larger optic thus obtaining a
dimmer image. By far the worst problem is the aberrations
created by the inherent misalignment of the smaller optical
elements .

Aberrations are phase distortions which prevent the

2
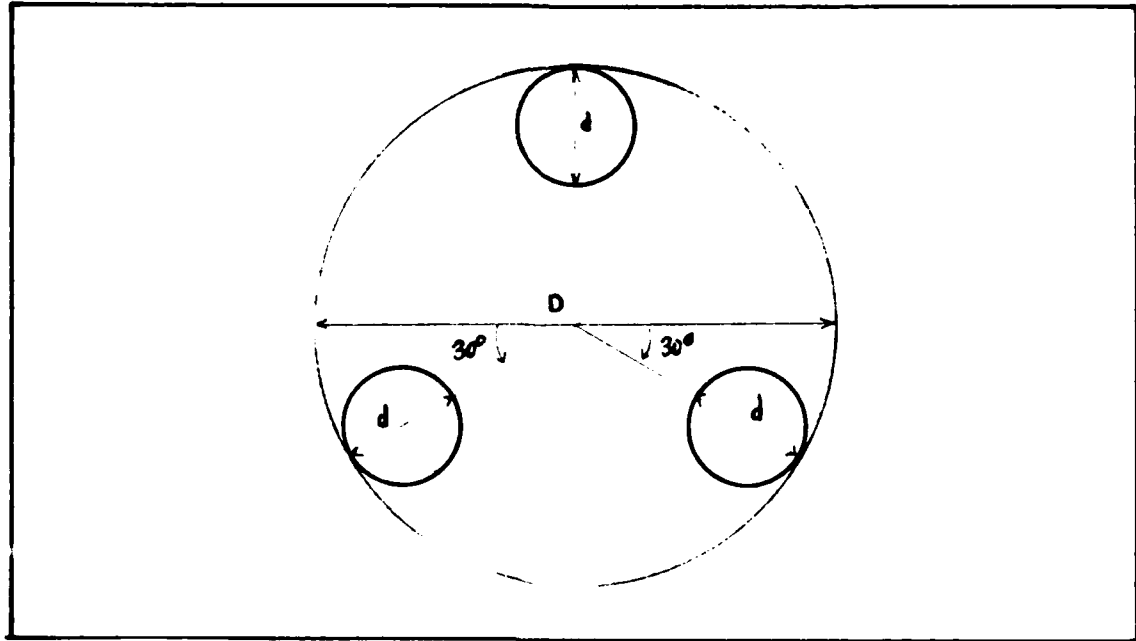
Figure 1.   Synthetic Aperture Geometry

wavefront exiting the imaging element from being perfectly

spherical.   This keeps the object wavefronts from being

focused to the ideal geometrical image point, thus

distorting the image (10:120).   These aberrations can

become so severe that the enhanced resolution obtained from

the synthetic aperture is destroyed by a blurred image.   In

order for synthetic apertures to be useful in optical space

systems, the aberration problem must be corrected.   One

way to undo the effects of aberrations is through the use

of holography.   Upatnieks and Leith first demonstrated the

feasibility of aberration correction of a single-lens

system using holography in 1965 (26:589).   In 1974 Kuzilin

and Sinston reported that they had successfully applied

this technique to a synthetic aperture (18:352). Since that time, holographic correction of aberrations has been the subject of considerable research. For the past three years the Air Force Institute of Technology (AFIT) has maintained ongoing research in this area. Detailed explanation of how holograms can correct aberrations as well as the intensity patterns produced by the synthetic aperture in Figure 1 can be found in these thesis efforts (15:6-21; 8:7-56).

Most holograms are recorded on photographic plates with a light sensitive emulsion (usually silver halide) on one side. High sensitivity, low cost, commercial availability, and stability after processing make fine-grain, silver halide, photographic emulsion a very desirable holographic medium (13:636). The requirement for a time consuming developement process (~8 hours), however, renders photographic plates useless for space systems where real time (less than seconds between recording and reading the hologram) aberration correction is needed. For this reason, the use of electro-optic materials such as lithium niobate ($LiNbO_3$), barium titanate ($BaTiO_3$) and bismuth silicon oxide ($Bi_{12}SiO_{40}$ or BSO) for holograms has been the thrust of recent research. An early demonstration of a near real time hologram using $LiNbO_3$ was reported by Chen in 1968 (3:223). These crystals exhibit what is called the "photorefractive effect" which results from a polarization change in the

4

crystal caused by a photo-induced charge transfer (12:199).
The most used figure of merit associated with hologram
formation in electro-optic materials is diffraction
efficiency. Diffraction efficiency is "the ratio of power
diffracted into one first-order wave to the power
illuminating the hologram" (5:224). The most recent
research effort conducted at AFIT established the
feasibility of using $LiNbO_3$ to correct aberrations but the
effort suffered from poor diffraction efficiency (8:57).

There are, however, drawbacks associated with using
electro-optic crystals. The most significant problem
associated with using these crystals for holograms is their
wavelength sensitivity. While fast and efficient
holograms can be recorded in these crystals at one
wavelength, the use of the same wavelength light will
destroy the existing hologram before it can be effectively
read out (3:224). One way to perform non-destructive
readout is by using different wavelength light (usually a
longer wavelength since the crystal is less sensitive at
longer wavelengths) (4:3390). The successful use of
electo-optic crystals for real time aberration correction
could be the key to deploying a synthetic-aperture optical
system.

Approach

This thesis effort was conducted in three stages.
First, the theory behind hologram formation in electro-

optic crystals was investigated. Second, a synthetic-
aperture optical system was designed which best depicted
how an actual space system would operate. Finally,
experiments were conducted to characterize the BSO crystal
used, then using this crystal, to correct single-lens
system and synthetic-aperture system aberrations.

II. <u>Theory</u>

<u>Overview</u>

In 1966 the photorefractive effect (first referred to as "laser damage effect") was first observed at Bell Laboratories (2:72). Since that time extensive research has been conducted on the photorefractive properties of electro-optic crystals. While a general explanation of the hologram formation process is well understood, there have been numerous works pertaining to the exact details of how charges migrate under certain conditions within the crystal (1:22; 4:3389; 6:1297; 9:223; 16:3279; 17:949; 24;1042; 25:5188; 27:3510; 28:264). This chapter consists of a general description of how holograms are formed in electro-optic crystals and a discussion of the two key parameters associated with synthetic aperture applications -- diffraction efficiency and hologram erasure rate. Since a BSO crystal was used in the experimental portion of this thesis effort, the latter sections relate specifically to the diffraction efficiency and hologram erasure rate of BSO crystals. An in-depth analysis of the theory involving grating formation in electo-optic crystals can be found in the thesis effort performed at AFIT by Captain Marciniak (21:5-90).

<u>Hologram Formation</u>

Assume that two coherent light beams of wavelength and intensities I and I are incident on the face of an

7

electo-optic crystal as shown in Figure 2.
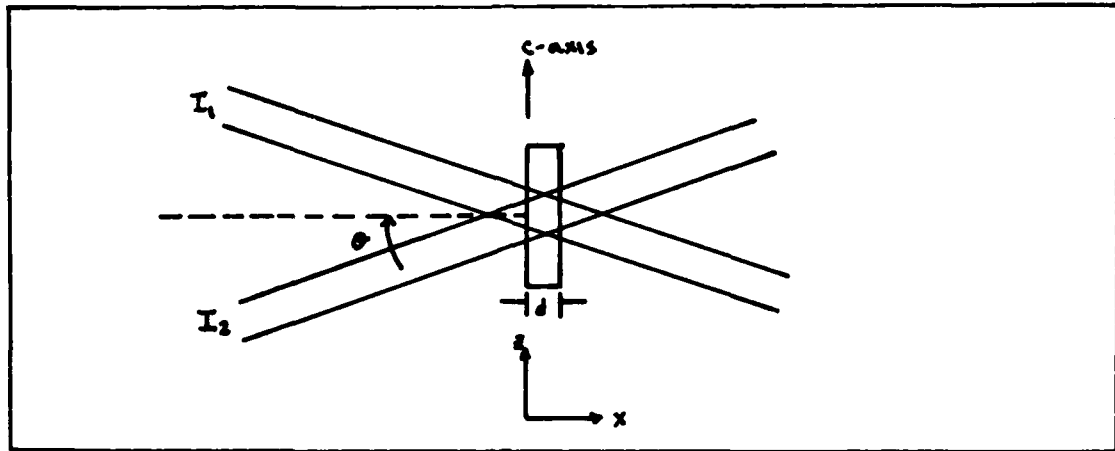
Figure 2.   Hologram Formation in Electro-optic Crystal

Let the bisector of the two beams be normal to the crystal face and the c-axis.   With this crystal orientation, the resulting interference fringes will be perpendicular to the c-axis.   The associated intensity pattern is:

$$I(z) = I_o(1 + m\cos Kz) \qquad (2)$$

where $I_o = I_1 + I_2$, m is the modulation ratio ($m = 2(I_1 I_2)^{1/2}/I_o$) and K is the spatial frequency ($K = 2\pi/\Lambda$).   The fringe spacing (Λ) is the distance between intensity maxima and is given by:

$$\Lambda = \lambda/2\sin\theta \qquad (3)$$

Assume that two types of charges exist in the crystal -- charges that can be photo-excited and an equal number of

8

charges that cannot be photo-excited. In the presence of the intensity distribution given in Eq (2), electrons are excited in the areas of illumination and migrate to the areas of no illumination where they become trapped. The migration mechanism can be diffusion, drift in an applied field, and drift due to photovoltaic field depending on the type of crystal used and the experimental setup. After migration, the resulting separation of charges generates a static electric field due to Poisson's equation. This field is parallel to the direction of the interference fringes. The strength of this static electric field depends on the number of charges which were photo-excited and the migration mechanism. Assuming no applied field, the static electric field is given by:

$$E(z) = -(K_B T/q) \; mK/(1+(K/K_o)^2) \; \sin Kz \qquad (4)$$

where $K_B T$ is the thermal energy of the lattice, q is the charge of the mobile charge carriers and K_o is a material constant related to the number density (N) of available charge carriers(7:423). The equation for the material constant K_o is:

$$K_o = (Nq^2/\epsilon \epsilon_o K_B T)^{1/2} \qquad (5)$$

where ϵ is the static dielectric constant and ϵ_o is the free-space electric permeability. In the above

9

expression for the light induced electric field, it is assumed that the diffusion length between trapping sites is much less than the spatial frequency of the intensity pattern. This static electric field then causes a change in the crystal's refractive index, $\Delta n(z)$, by the linear electro-optic (Pockel's) effect. The strength of $\Delta n(z)$ will depend on the symmetry of the electro-optic tensor related to the type of crystal used and the light induced static electric field. This modulation of the crystal's index of refraction produces a volume phase grating within the crystal thus forming a hologram.

Diffraction Efficiency and Erasure Rate for BSO

As previously mentioned, the strength of the crystal's refractive index changes. Thus, its diffraction efficiency is related to the crystal orientation. BSO is a paraelectric, electo-optic and photoconductive material having the cubic point group symmetry $\bar{4}3m$ (12:240). Crystals of this type are optically isotopic until an electric field is applied where they become birefrengent due to the non-vanishing Pockel's coefficient. The orientation, dimensions and direction of the principle coordinate system (PCS) of the BSO crystal used in this thesis effort is shown in Figure 3. With vertically polarized light incident on the 110 crystal face, the direction of the interference fringes indicate that the resulting static electric field will have both an x and y

10
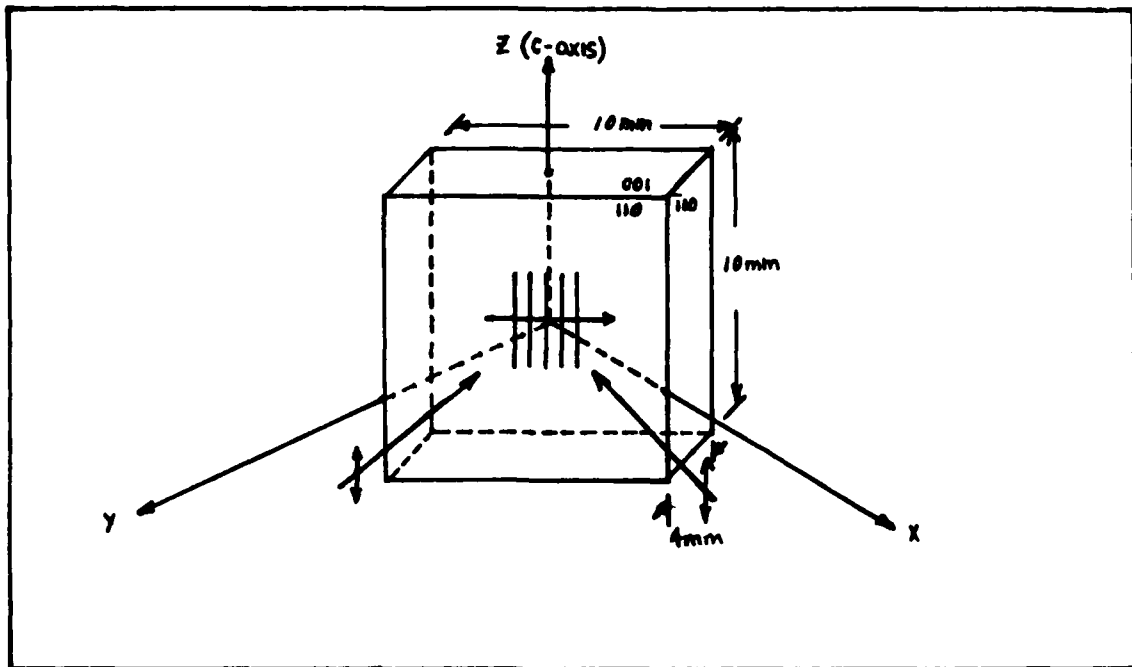
Figure 3. BSO Crystal Dimensions and Orientation

component. For the case of no applied field, diffusion
will be the dominate charge migration mechanism and the
resulting refractive index change will be

$$\Delta n = n^3 r_{41} E \qquad (6)$$

where n is the crystal's refractive index, r_{41} is the
Pockel's coefficient and E is the magnitude of the static
electric field. The above orientation provides for
maximum diffraction efficiency since there is no gain
between the beams entering and exiting the crystal.
Another criteria for optimum diffraction efficiency is for
the ratio of the writing beams to be equal to one (12:267).

11

Assuming no gain and $I_1 = I_2$, the equation for diffraction efficiency becomes:

$$\eta = (\delta E_p d/2)^2 \ (E_q/(E_o + E_q))^2 \ \exp(-\alpha d) \qquad (7)$$

where α is the crystal's absorption coefficient and d is the crystal's thickness(22:133).

After the hologram is recorded and the writing beams shut off, the BSO is capable of storing (dark storage) the hologram for approximately 30 hours (23:3690). To determine the time constant of the diffracted beam, the erasure rate of the hologram must be determined. To do this the static electric field must be calculated with respect to time as well as position. In the absence of applied field, the erasure rate is mainly due to the drift in the photo-induced static field (23:3688). Assuming the cross sections of the trapping sites are all equal and the read beam intensity uniform, the erasure rate can be expressed as:

$$t_e = (N/q_o)(K^2 L_o'^2 + 1)/(K^2 L_o'^2) \qquad (8)$$

where N is the number of photo-excited charges, q_o is the rate at which the photo-excited charges are generated, and L_o' is the diffusion length. The generation rate (q_o) is

determined by:

$$q_o = \Phi \alpha I_o / h\nu \qquad (9)$$

where Φ is the quantum efficiency for exciting a charge carrier, I_o is the read beam intensity and $h\nu$ is the photon energy. The diffusion length is given by:

$$L'_D = (D\tau)^{1/2} \qquad (10)$$

where D is the diffusion coefficient and τ is the free carrier lifetime ($\tau = 1/\gamma_R N$; $\gamma_R \equiv$ carrier recombination constant).

With complete knowledge of the crystal's material characteristics, the diffraction efficiency and erasure rate can be calculated using the above equations. Without all the crystal characteristics the theoretical calculations of diffraction efficiency and erasure rate are estimates which may or may not agree with the experimental data taken.

III.   Experimental Apparatus

Overview

The equipment used for the following experiments were of commercial quality and obtained from the existing inventory of AFIT's laboratory. All the optical systems used were of original design and were assembled on a 12 x 4 foot shock isolated optics table.   Since holograms in the BSO had to be recorded at one wavelength and read out at another, two light sources were used.   The light sources for each experiment were a Spectra Physics model 2020-03 Argon-ion laser equipped with an inner-cavity etalon tuned for an output wavelength of 488 nm and a Hughes model 4142 helium neon (HeNe) laser.   The first optical system covered in this chapter dealt with determining the BSO crystal characteristics.   The following sections detail the setup for the single lens aberration correction and synthetic aperture aberration correction experiments.

Experiment 1 Optical System

Figure 4 shows a diagram of the optical system used in the first experiment.   The Argon-ion laser provided the monochromatic (488 nm or blue) light beams for recording the hologram within the BSO crystal.   A periscope was used to position the blue beam 17 cm above the table.   The beam was divided by a variable beam splitter and reflected toward the crystal by two mirrors mounted on shock
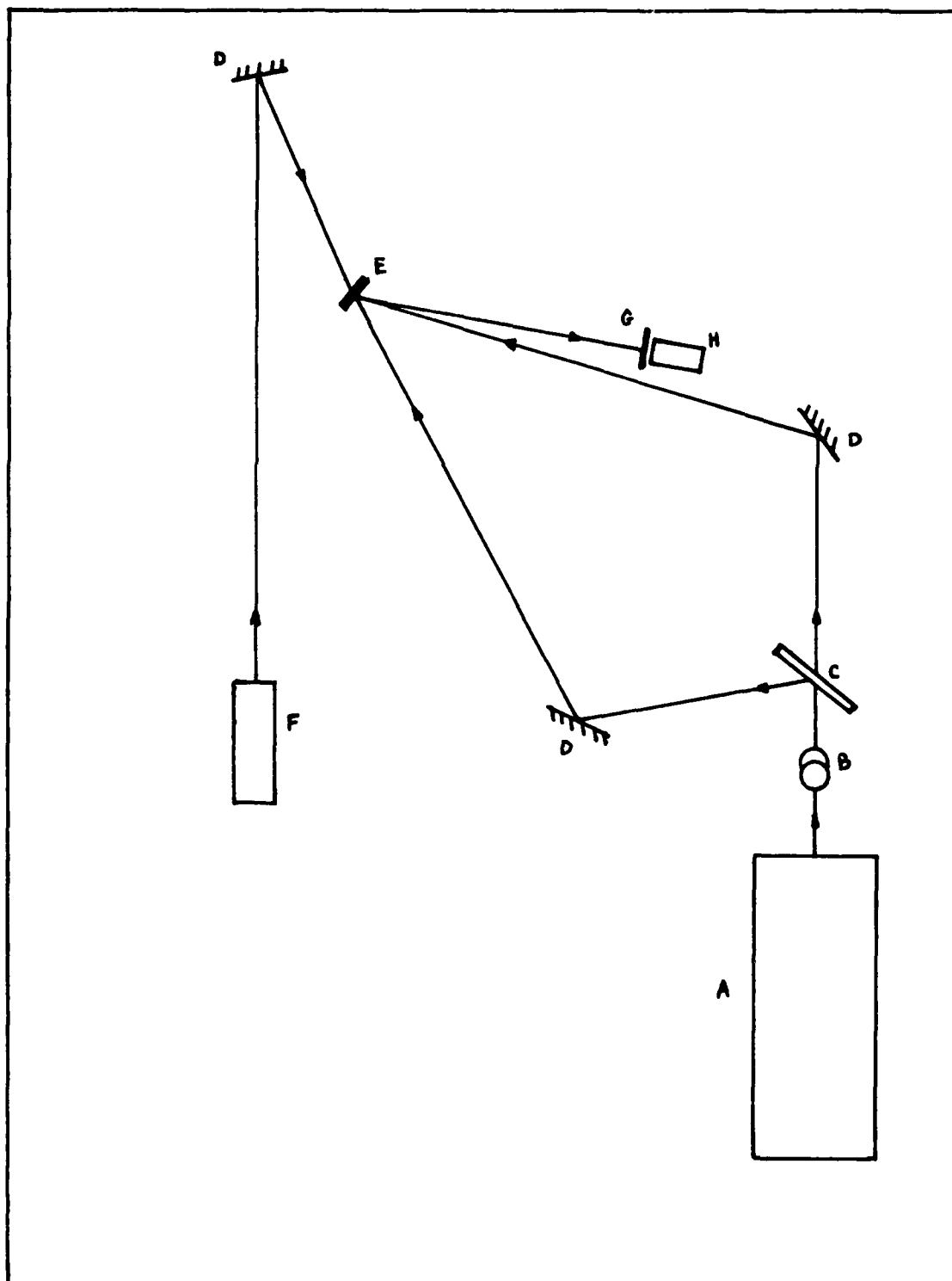
14

Figure 4. Schematic of Experiment 1 Optical System
(A table providing the description and
characteristics of each system element
is presented on page 20)

absorbing poles. The crystal was positioned at a point where the bisection of the two writing beams was normal to the 110 crystal face.   The mount holding the BSO crystal was equipped for adjustments in the x (along te optical axis), y (horizontal), and z (vertical) directions as well as angular rotation in the plane containing both writing beams.   The HeNe laser provided the longer wavelength (632.8 nm) light for the read beam.The HeNe laser was positioned parallel to the Argon-ion laser but on the opposite end of the table.   From this location the read beam could be reflected into the back of the crystal at the Bragg diffraction angle for 632.8 nm light.   A radiometer was placed at the appropriate point to obtain the power of the diffracted red beam.   The radiometer was equipped with an 110 nm bandwidth filter centered at 634 nm which blocked the stray intensity of the blue writing beams.

Experiment 2 Optical System

The optical system depicted in Figure 5 was used for the aberration correction of a single lens.   In order to image an Airy pattern through the objective lens, the source beams were filtered, expanded and collimated into a plane wave.   A standard spatial filter mount containing a 10x microscope objective and a 25 μm pinhole was used in conjunction with an 86 mm focal length collimating lens to produce the blue plane wave.   The blue beam was split into an object and reference beam by a variable beam splitter

16

Figure 5. Schematic of Experiment 2 Optical System
(A table providing the discription and
characteristics of each system element
is presented on page 20)

which could be adjusted to allow the object and reference beam intensities to be equal. The reflecting mirrors directed the object and reference beams toward the BSO crystal (using the same mount as in Experiment 1) which was, again, positioned with the bisector of the writing beams normal to 110 crystal face. A high quality plano-convex lens (f = 146 cm) was placed in the path of the object beam with an iris positioned as close to the front of the lens as possible. Along with its tilt adjustments, the objective lens was mounted to facilitate adjustment in the x, y, and z directions while the iris could only be adjusted in the y and z directions. Another 146 cm focal length lens was placed in the path of the reference beam in order to focus the 1.5 cm diameter beam within the 1 cm^2 crystal. Microscope objectives were positioned at the focal point of each lens for viewing purposes. A 35 mm camera attached to a tripod was used to photograph the image obtained from the microscope objectives.

The HeNe laser was carefully positioned to allow the red beam to travel down the same path as the blue beam. The red plane wave was obtained from a 40x microscope objective, 25 μm pinhole and a Jodon collimating lens which could be fastened onto the spatial filter mount.

Experiment 3 Optical System

A schematic of the optical system used in Experiment 3 is shown in Figure 6. The blue beam from the Argon-ion
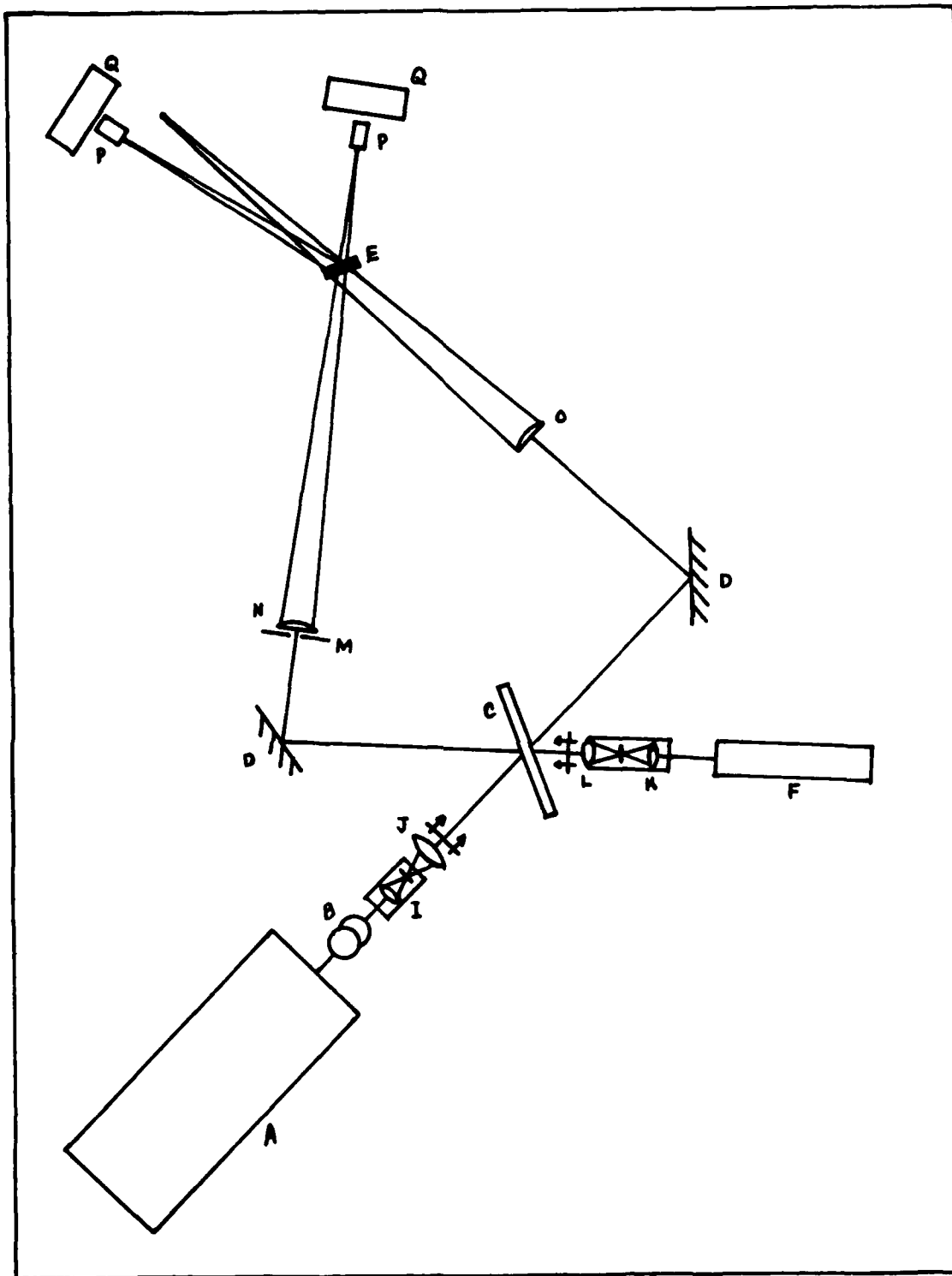
18

Figure 6. Schematic of Experiment 3 Optical System
(A table providing the description and
characteristics of each system element
is presented on page 20)
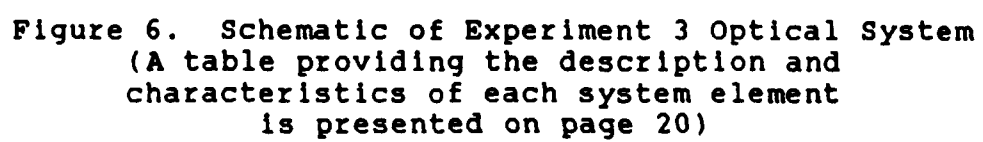
Table I

Elements of the Optical Systems

Element	Description	Make & Model	Focal Length	Comments
A	Laser	SP 2020-03	-	Argon-ion
B	Periscope	NRC-675	-	-
C	Variable Beam Splitter	NRC	-	-
D	Mirror	NRC	-	2" dia.
E	BSO crystal	Sumitomo	-	10x10x4mm
F	Laser	HAC-4142	-	HeNe
G	Filter	Oriel: 53090 #9	-	634nm center 110nm BW
H	Radiometer	United Detector Technologies	-	-
I	Spatial Filter	Jodon	-	10x 25μm
J	Collimating Lens	Unknown	86mm	Bi-convex
K	Spatial Filter	Jodon	-	40x 25μm
L	Collimating Lens	Jodon	-	Screw in Type
M	Iris	Unknown	-	4.5mm dia.
N	Objective Lens	Ealing: 34-2834	1460mm	Plano-Convex
O	Focusing Lens	Ealing: 34-2834	1460mm	Plano-Convex
P	Microscope Objective	Bausch & Lomb	-	40x

Table I (continued)

Element	Description	Make & Model	Focal Length	Comments
Q	35mm Camera	Pentax K-1000	–	135 ASA B&W Kodak film
R	Expanding Lens	Unknown	86mm	Bi-convex
S	Collimating Lens	Kodak Telephoto	1524mm	Surplus Lens
T	Synthetic Aperture Lens	Ealing: 34-2834	1460mm	Plano-Convex
U	Mirror	NRC	–	4" dia.
V	Focusing Lens	Unknown	140mm	Plano-Convex
W	Telescope	National Scientific	–	4x 10x

laser was filtered and collimated as in Experiment 2 to produce a plane wave. The blue plane wave was divided by a variable beam splitter. The object beam was reflected by two mirrors then expanded by an 86 mm focal length lens. A large diameter (f=1524 mm) lens was positioned to recollimate the beam into a plane wave which could uniformly illuminate the synthetic aperture. The synthetic aperture consisted of three high quality plano-convex lens positioned as shown in Figure 1 . The two lower lenses were mounted on shock absorbing poles and the upper lens was mounted on a magnetic base. Each lens mount was equipped for adjustment in the x, y, and z directions as well as tilt. Two sets of mirrors reflected the three emerging light beams toward the BSO crystal which was mounted and oriented as in the previous experiments. The reference beam was reflected by four mirrors toward the BSO crystal. A focusing plano-convex lens (f=140 mm) was positioned in the reference beam path to focus the reference beam within the edges of the 1 cm² BSO crystal. A telescope equipped with a 4x microscope objective and 10x eyepiece was mounted on a magnetic base. This allowed movement of the telescope to either the combined focal point of the diffracted beam or the focal point of the reference beam. The system impulse response was viewed through a 40x microscope objective positioned at the focal point of the synthetic-aperture. The same 35 mm camera used in Experiment 2 provided photographs of the images

22

obtained from the microscope objective and telescope.

The red beam from the HeNe laser was positioned behind the beam splitter and aligned such that the red beam was superimposed upon the blue beam.   The red plane wave was produced in the same manner as in Experiment 2.

IV. Experimental Procedure and Results

Overview

The experimental portion of this thesis effort was
designed to determine the characteristics of the BSO
crystal; and from the results of this characterization, use
the BSO crystal to correct synthetic-aperture aberrations.
The designs of the optical systems in the latter two
aberration correction experiments were developed to
coincide, as closely as possible, with the operation of a
synthetic aperture in space. For this reason, a section
detailing the author's conceptual synthetic-aperture space
system design has been included in this chapter and will be
covered first. The next section will detail the procedure
of the BSO characterization experiment and be immediately
followed by a section describing the results of the
characterization. This format will be followed until the
results of the synthetic-aperture aberration correction
experiment are presented at the end of this chapter.

Conceptual Synthetic Aperture Space System

Figure 7 provides a schematic of the author's
conceptual synthetic aperture space system. The
individual synthetic aperture elements are a meter in
diameter and the center to center spacing between each
element is three meters. In this arrangement, the
resolution of a single optic with a diameter of

24
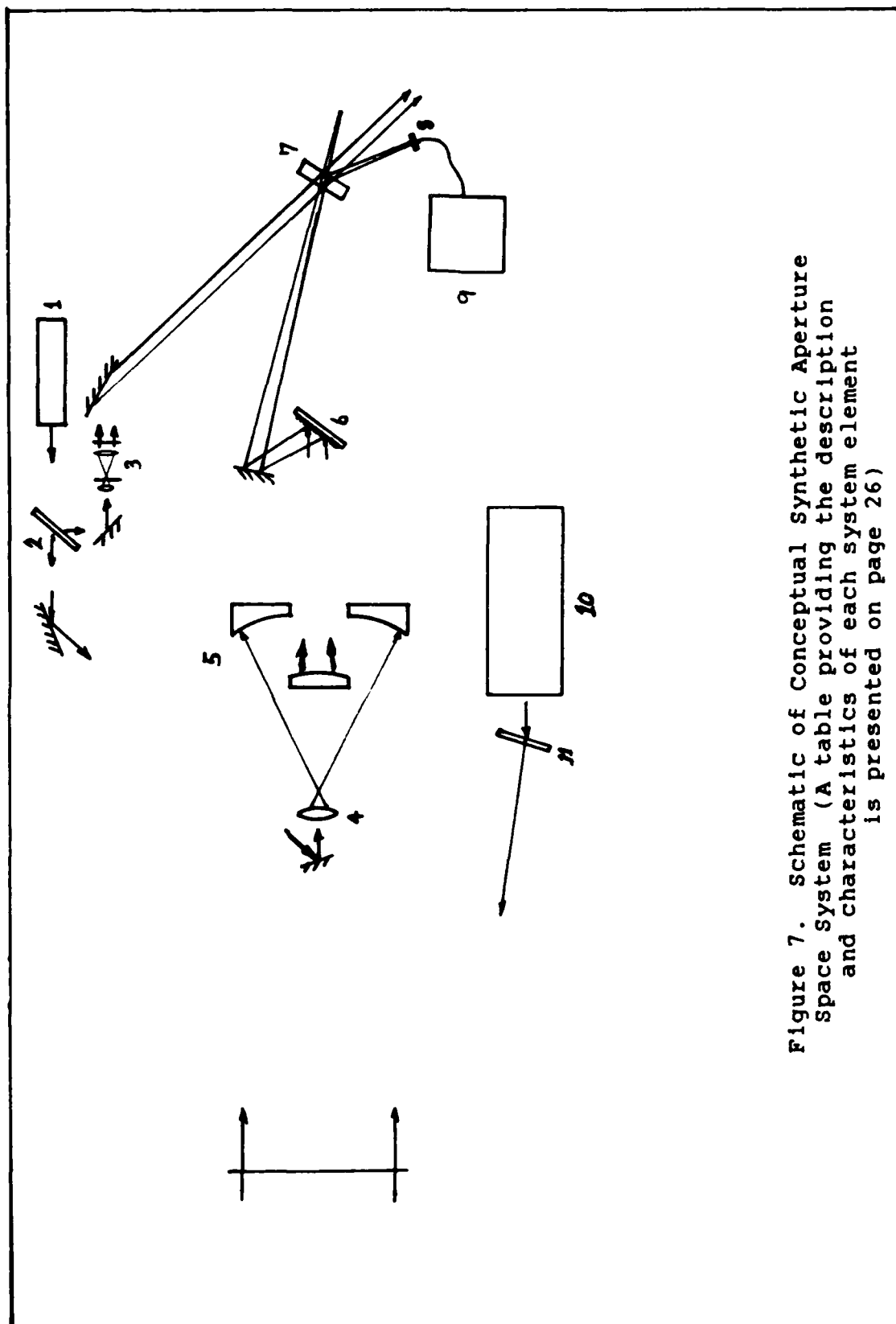
Figure 7. Schematic of Conceptual Synthetic Aperture Space System (A table providing the description and characteristics of each system element is presented on page 26)

Table II

Elements of the Conceptual Synthetic-Aperture Space System

Element	Description
1	Laser operating at λ_1
2	Beam Splitter
3	Plane Wave Generating Optics
4	Diverging Lens
5	Synthetic-Aperture Reflective Optics
6	Diffraction Grating
7	Electro-Optic Crystal
8	Optical Filter & Detector
9	Signal Processor
10	Laser Operating at λ_2
11	Beam Steering Device

approximately five meters can theoretically be obtained.
Reflective optics are utilized to minimize the aberrations
as much as possible. The use of an electro-optic crystal
as a holographic recording medium requires that the
hologram be recorded at one wavelength and read out at a
longer wavelength. A laser operating at λ_1 is used to
record the synthetic-aperture aberrations within the
crystal. The laser beam is split into a reference plane
wave and an object wave. The object wave is diverged into
a large spherical wave which is focused by the synthetic
aperture. A highly reflective diffraction grating is
placed in the path of the object beam to diffract the
different wavelength light at the appropriate angles for
entering the crystal. This is an active system which uses
a laser (operating at wavelength λ_2) and a beam steering
device to illuminate the target in question. Since the
target will be several kilometers away, the reflected
object wave will be spherical at first then slowly diverge
to a plane wave before it reaches the synthetic aperture.
This plane wave is focused by the synthetic aperture and
diffracted by the grating to enter the crystal at the Bragg
diffraction angle for λ_2 ($\lambda_2 > \lambda_1$). The reconstructed wave
is diffracted onto a detector equipped with a filter which
blocks any stray light incident on the detector. The
detector output is signal processed to determine if the
target is a threat or a decoy.

There are two problems associated with this design.

The light rays from the target are incident on the synthetic aperture at different angles than the light rays used to record the hologram. This could cause the target beam to enter the crystal at the wrong angle thus hindering the aberration correction. One way to minimize this problem is to enable slight adjustments of the mirror located in the target beam path in relation to the range of the target. The more obvious problem with this design is the location of the mirror and diverging lens which blocks a portion of the target beam. This might not be a significant problem if the physical size of the mirror and lens is small in comparison to that of the synthetic aperture.

The system design presented here is one way in which a synthetic aperture might be deployed in space. The author realizes that this design can, at best, be described as preliminary.

Experiment 1: Procedure

The optical system shown in Figure 4 was constructed. Marrakchi and Huignard determined in their experimental work that for no applied field, the diffraction efficiency for BSO was greatest when the hologram fringe spacing was less than one micron (22:131). From Eq (3) a fringe spacing (Λ) of one for 488 nm wavelength light relates to an angular seperation between the writing beams of 28.2°. Therefore, in order for to be less than one micron, the mirrors and crystal were positioned for a 30° angular

28

seperation between the writing beams. The angle at which

the HeNe read beam needed to enter the crystal was also

determined from Eq (3). Since BSO is very optically

active, the diffraction efficiency (for no applied field)

saturates at writing beam intensities as low as 300

$\mu W/cm^2$ (22:135). The writing beam intensities were kept

equal and above 10 mW/cm^2 during the experiment. The

crystal was probed with the red beam while simutaneously

being illuminated by the blue writing beams. This allowed

the highest power of the diffracted red beam to be measured

with the radiometer for that particular writing angle. By

moving the crystal closer to or farther away from the

reflecting mirrors, the writing angle could be varied.

Measuring the power of the diffracted red beam at different

crystal positions provided the diffraction efficiency

versus fringe spacing characteristics of the crystal.

The erasure rate of the stored hologram was determined

by turning off the writing beams and allowing the read beam

to erase the hologram. For a fringe spacing of 3 μm,

measurements of the diffracted power were taken at five

second intervals to determine the diffraction efficiency

versus time (erasure rate) characteristics of the BSO

crystal.

Experiment 1: Results

The diffraction efficiency versus fringe spacing curve

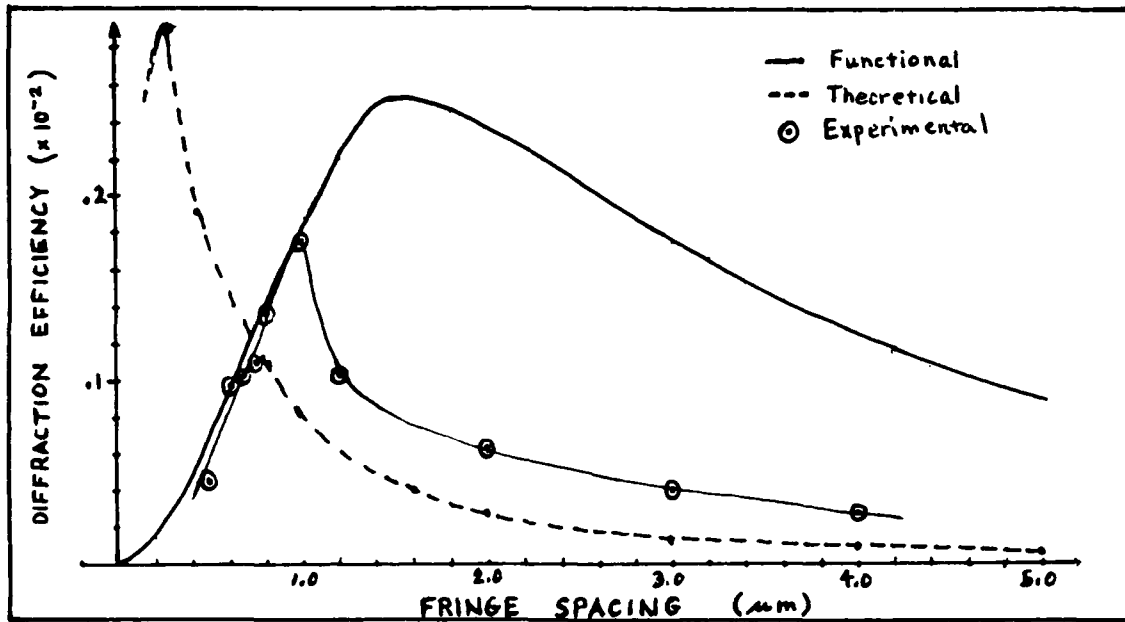for the BSO crystal is shown in Figure 8. The maximum

Figure 8. Plot of Diffraction Efficiency vs Fringe
Spacing for BSO (Functional curve from 6:1300
and the theoretical curve from Eq 7)

diffraction efficiency was obtained at a fringe spacing of

0.96 μm which relates to a $29.3°$ angular seperation of the

writing beams. The experimental curve has the same

functional form as the theoretical curve but peaks at a

lower value of diffraction efficiency and a different

fringe spacing. The functional relationship between

diffraction efficiency and fringe spacing is also shown in

Figure 8. The theoretical curve was plotted from Eq (7)

with $N = 1 \times 10^{21}$ m^{-3} , $\alpha = 2.2 \times 10^{-2}$ m^{-1} , $n = 2.54$ and

$r_{41} = 1 \times 10^{-12}$ m/V. The lower experimental diffraction

efficiency peak was caused by lower actual values of the

charge density and electro-optic coefficient related to the

BSO crystal used in this effort. The fact that the two

curves peaked at different fringe spacings is somewhat

harder to expain.   It is believed that the seperation of

the two peaks was caused by mechanical vibrations of the

laser which resulted in a slightly unstable fringe

pattern incident on the crystal.   Similar results of

diffraction efficiency versus fringe spacing for a BSO

crystal (same manufacturer as crystal used in this effort)

were obtained in the thesis research of Captain Leatherman

(19:49). Since the functional form of the two curves is the

same, the experimental data is taken to be an accurate

account of the diffraction efficiency versus fringe spacing

characteristics of the BSO crystal used in this thesis

effort.

Figure 9 depicts the erasure rate of the BSO crystal.

Both the theoretical and experimental curves reflect a

decaying exponential.   The theoretical curve starts at a

higher diffraction efficiency and decays at a faster rate.

The reason for both phenomeon is the theoretical points

were obtained for a BSO crystal which had 3 kV applied

voltage.   The applied voltage increases the crystals

change in refractive index thus increasing the diffraction

efficiency.   The charge mobility of the crystal is also

enhanced by the applied voltage thereby allowing the

hologram to erase faster.   With no applied voltage, the

charges migrate slower.   This is reflected by the

experimental curve since the diffraction efficiency did not
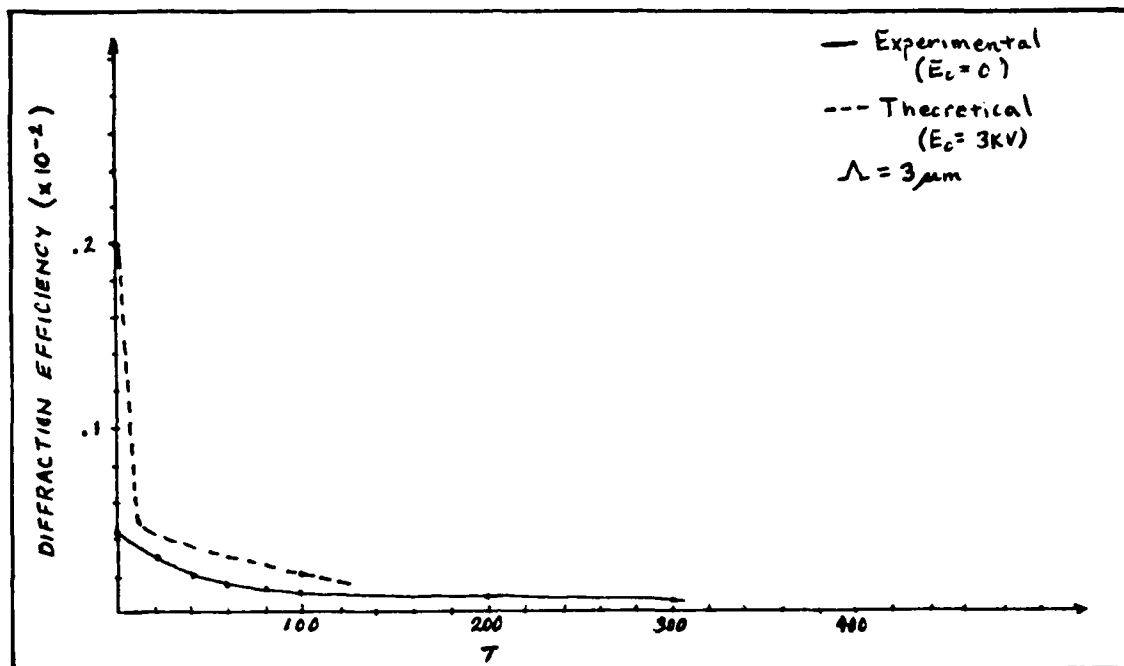
fall to the $1/e^2$ point for at least 300 seconds.

31

Figure 9. Plot of Hologram Erasure Rate for BSO
(Theoretical curve from 23:3687)

Experiment 2: Procedure

Using the results of Experiment 1, the optical system

depicted in Figure 5 was assembled with a 29° angular

seperation between writing beams. The objective lens was

positioned where the largest object beam diameter possible

would pass through the crystal and still have the focal

point within the optic table boundaries. The object and

reference beam paths were set at 126 cm. The iris

positioned in front of the objective lens was opened to a

diameter of 4.5 mm. Alignment of the objective lens

produced an image, from the microscope objective, of the

system Airy pattern impulse response. Figures 10 and 11

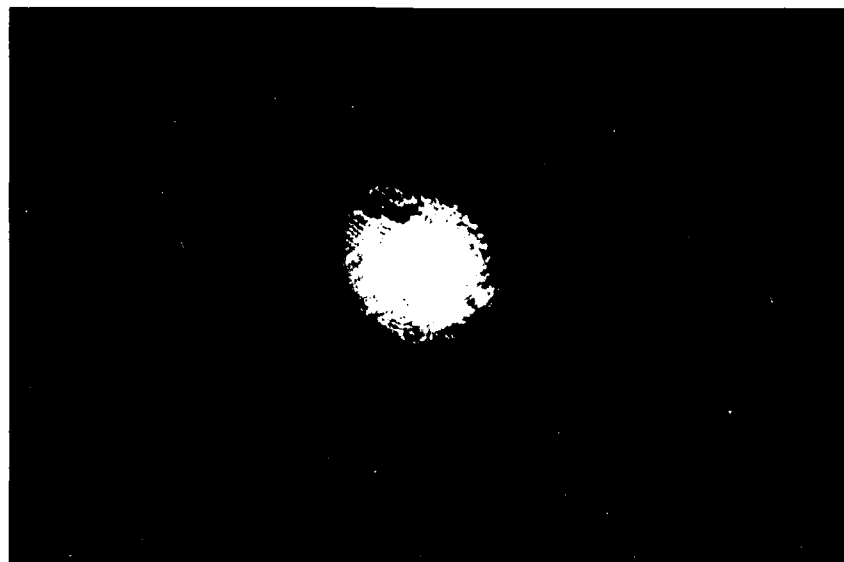show the Airy pattern impulse response for the blue and red

32

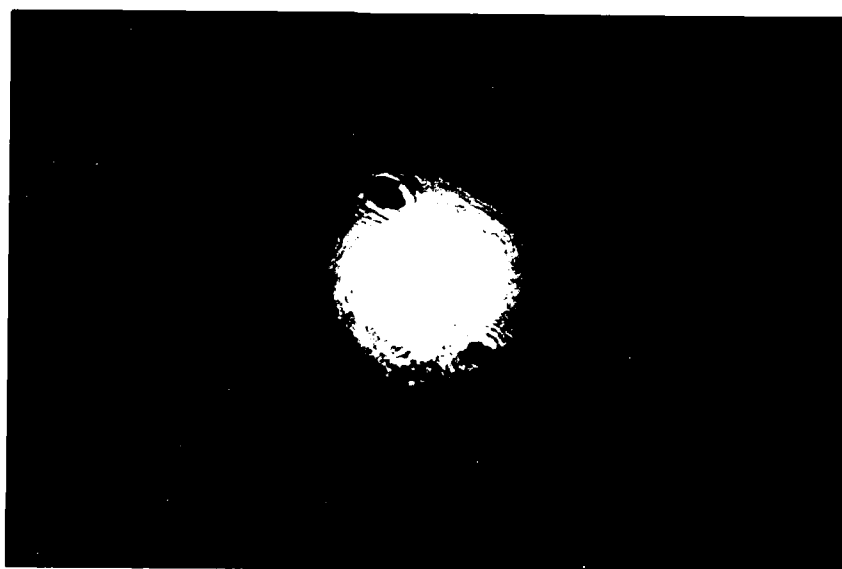Figure 10.   Single Lens System Impulse Response
for Blue Beam

Figure 11.   Single Lens Syetem Impulse Response
for Red Beam

33

beams, respectively. The reference beam was focused to a
beam diameter which filled the front surface of the crystal
without hitting the edges. A hologram of the aligned
system was recorded and then the blue beams were shuttered
off. After blocking the reference path, the red beam was
turned on. In order for the readout beam to enter the
crystal at the correct angle, the crystal was slowly
rotated until the diffracted beam emerged. A microscope
objective was positioned at the diffracted beam focal point
and Figure 12 depicts the image of the systems diffracted
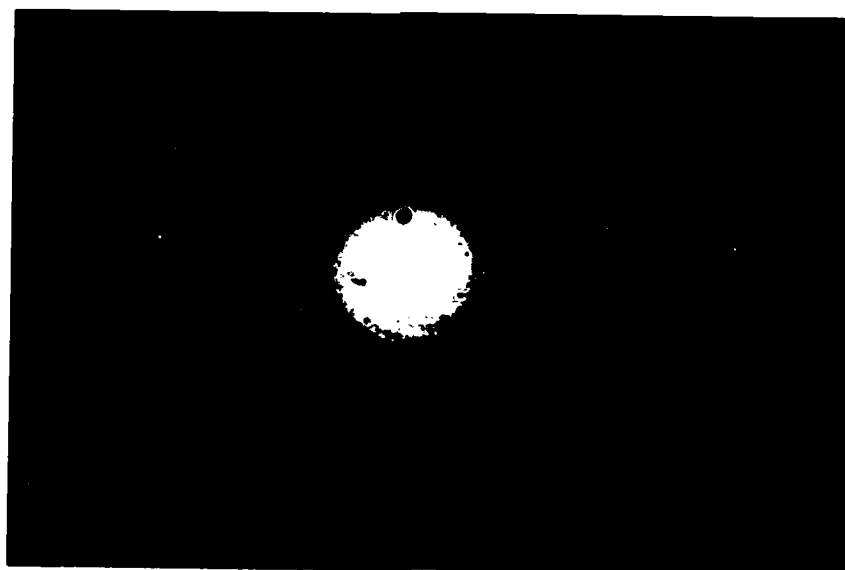impulse response. This figure reflects the best

Figure 12. Reconstruction of Aligned Single Lens Ststem

holographically obtainable and provides a benchmark with which the aberration correction quality can be measured.

The system was aberrated by moving the iris horizontally (~2 mm) off the optic axis. The aberrated impulse response is shown in Figure 13. With the HeNe laser off, a hologram of the aberrated system was recorded. the diffracted or reconstructed wave was obtained using the same technique as before.

Experiment 2: Results

The reconstructed impulse response is depicted in Figure 14. The reconstruction has clearly restored the central maxima and the first minima of the aberrated Airy pattern. About half of the first maxima is dimly visible. Since the diffracted beam of the aligned system was also dim, the faintness of the two beams can be attributed to low diffraction efficiency. This problem could be solved with the application of a voltage across the crystal. The missing half of the first maxima in the reconstructed impulse response is due to the red readout beam focusing at a slightly different focal point than the blue (chromatic aberrations). Repositioning the crystal closer to the objective lens would have enhanced the reconstruction because the different color beams would have had less distance in which to seperate. This, however, could not physically be achieved within the table dimensions and have the optimum writing angle between the recording beams.
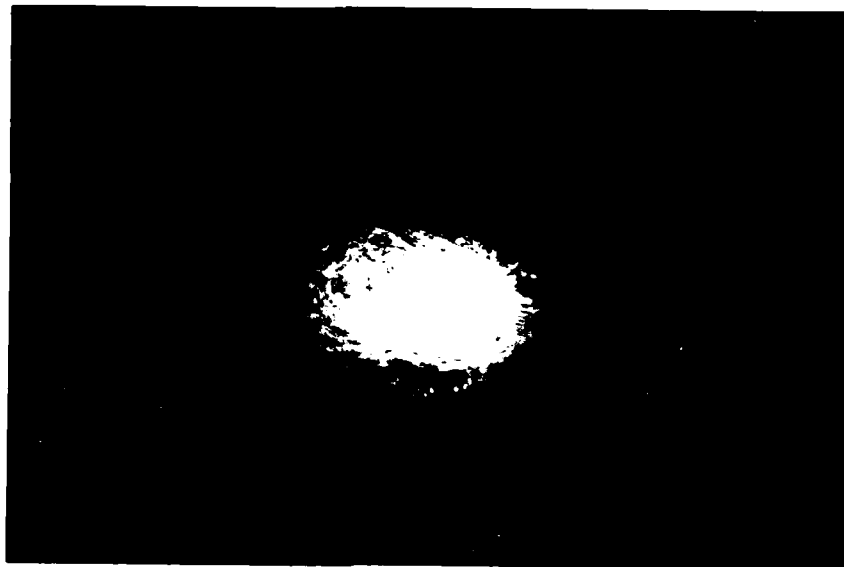
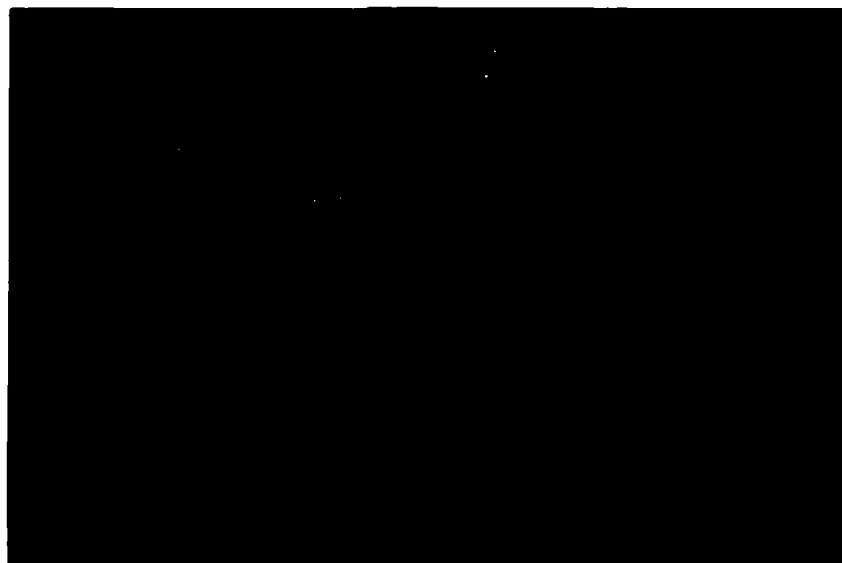Figure 13.   Aberrated Single Lens System Impulse Response

Figure 14.   Reconstruction for Aberrated Single Lens
System Impulse Response

Experiment 3: Procedure

The experiment began by constructing the optical system shown in Figure 6. The path length of both the object and reference beams was set at 470.5 cm. The angular seperation of the writing beams was 30°. The determination of a plane wave output from the big collimating lens was made using the shear-plate interfermetric analysis described by Malacara (20:105-148). The synthetic aperture was aligned in accordance with the synthetic-aperture alignment technique of Gill (8:61-64). The intensity patterns of the system impulse response for the blue and red beams are shown in Figures 15 and 16.
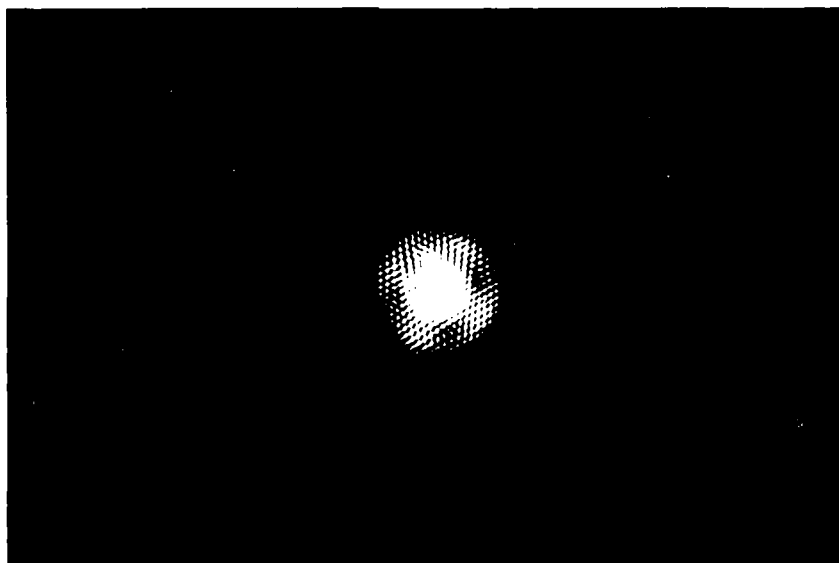
Figure 15. Synthetic Aperture System Impulse Response
for Blue Beam
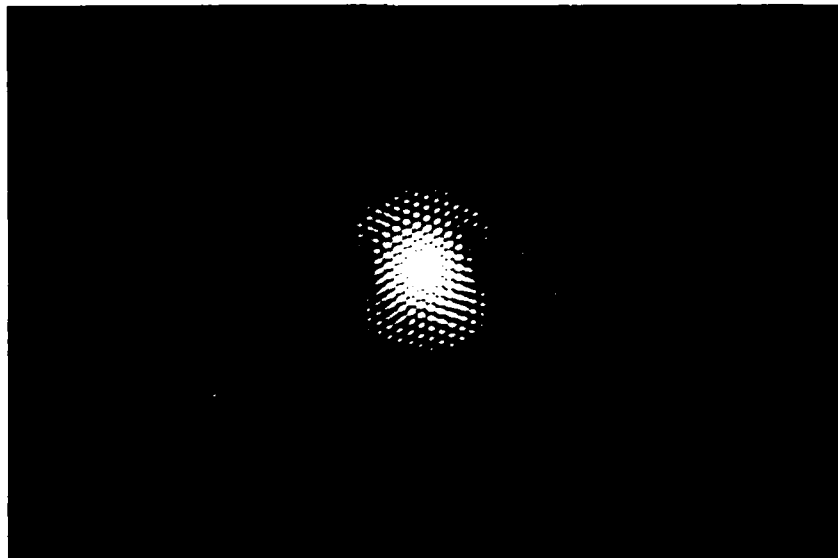
Figure 16. Synthetic Aperture System Impulse Response
for Red Beam

These impulse responses suffered from slight stigmatic

aberrations in the two lower synthetic-aperture elements.

The alignment of the synthetic aperture was repeated

several times but slight aberrations from the two lower

lenses persisted.

Other problems were encountered. In order to get all

three synthetic-aperture beams inside the crystal surface

area, the crystal had to be positioned close to the

synthetic-aperture focal point. This meant that the

individual beam diameters intersecting the crystal were

very small which caused the grating area to also be small.

The effective area of the grating was reduced even further

when the crystal was rotated to accept the readout beam.
The mirrors directing the synthetic-aperture beams toward
the crystal were repositioned to decrease the angular
seperartion of the beams.   This enabled the crystal to be
moved closer to the synthetic aperture thus allowing the
largest individual beam diameters to intersect the crystal.
The chromatic aberrations of the synthetic aperture
created the most significant problem.   The farther the
object beams traveled the farther the two beams separated.
By the time the beams reached the crystal, the red beams
were offset inside the blue beams.   The red beam was
diverged at the source under the pretense of slightly
increasing the red beams focal point to equal the blue beam
focal point.   This might have worked except the divergence
of the red beam decreased the intensity at the crystal to
the point where the diffracted beam was not visible.
Another problem was experienced with the reference beam.
The lens used to focus the reference beam in Experiment 2
was needed for the synthetic aperture and the only other
plano-convex lens available had a focal length of 140 mm.
The reference beam needs to be as aberration free as
possible in order to achieve quality reconstruction.   The
focusing lens used was aligned to produce an undistorted
Airy pattern but the short focal length caused the crystal
to introduce aberrations in the reference beam.   An iris
positioned in front of the focusing lens would reproduce
the undistorted Airy pattern but the beam was stopped down

39

to the point that the beam would not cover the three synthetic-aperture beams. Figure 17 shows the reference beam Airy pattern without entering the crystal and Figure 18 depicts the reference beam Airy pattern after intersecting the crystal. A hologram was recorded with the blue writing beams but the above problems had severe affects on the quality of the reconstruction wave.

Experiment 3: Results

Figure 19 depicts the reconstruction wave obtained from the above procedure. The reconstruction does not resemble either of the impulse responses shown in Figures 15 and 16. The low diffraction efficiency mentioned in
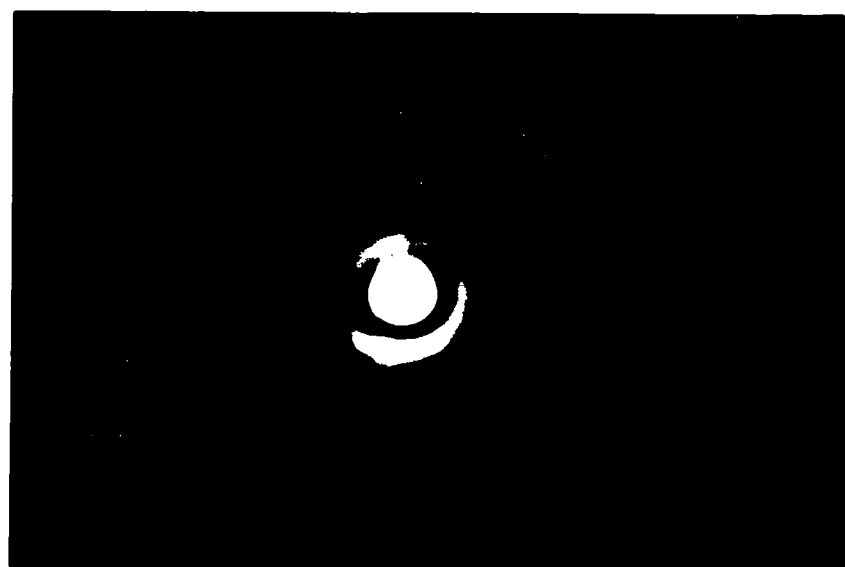

Figure 17.   Reference Beam Airy Pattern without
Intersecting Crystal
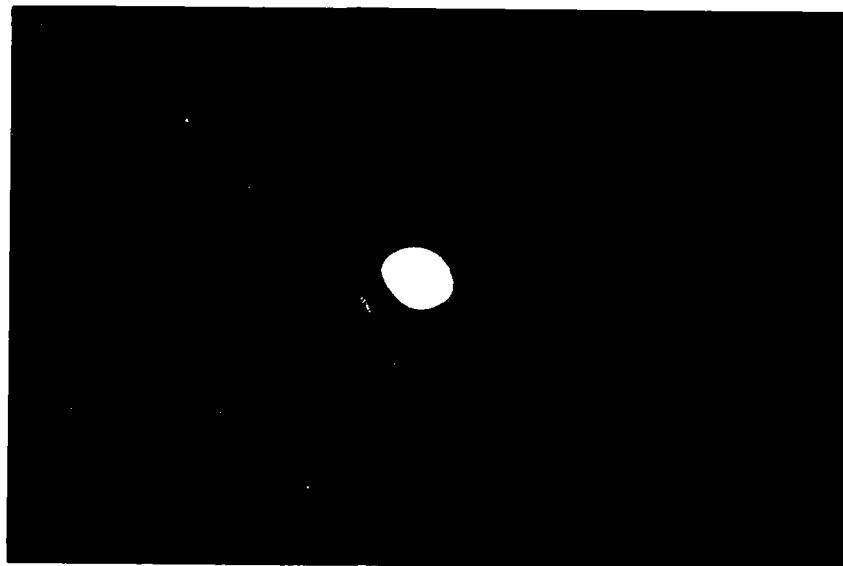
Figure 18. Reference Beam Airy Pattern after
Intersecting Crystal
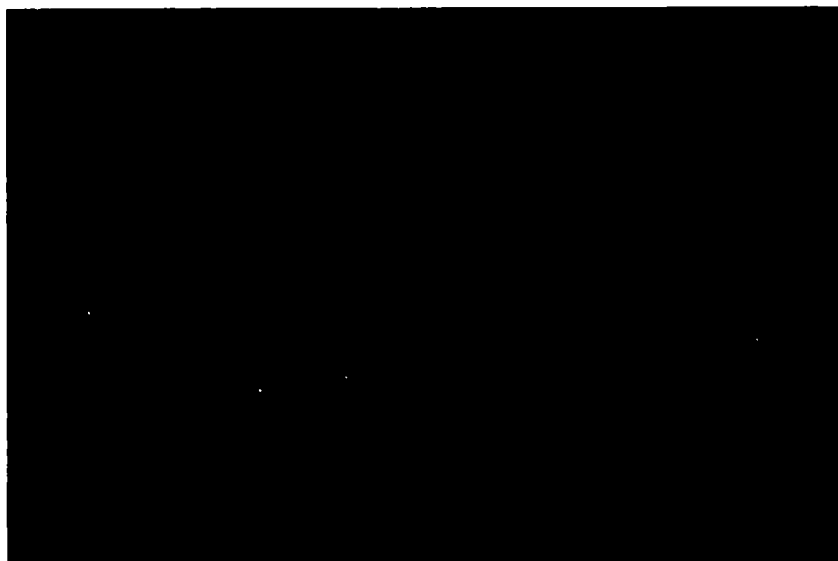
Figure 19. Diffracted Synthetic Aperture System
Impulse Response

Experiment 2 became an even worse problem in this
experiment as evidenced by the extremely faint
reconstruction.   The diffracted beams could only be viewed
with the help of a telescope.   The poor reference beam
quality and the chromatic aberrations were problems that
made aberration correction for the synthetic aperture
impossible.   A longer focal length lens to focus the
reference beam would have helped the reconstructed impulse
response but something must be done to create a common
focal point for the red and blue object beams before
aberration correction for this synthetic-aperture design
can be achieved.

V. Discussion and Recommendations

Discussion

This thesis effort was designed to determine the effectiveness of using electro-optic crystals to correct synthetic-aperture aberrations. Using the BSO crystal characteristics obtained in Experiment 1, successful real time (40 seconds between reading and writing) aberration correction for a single lens was performed in Experiment 2. This experiment suffered slightly from two problems which were magnified in Experiment 3. Poor diffraction efficiency and different focal points for the red and blue object beams rendered the successful correction of synthetic- aperture aberrations impossible.

The application of a voltage across the crystal would greatly enhance its diffraction efficiency. Efficiencies as high as 20% have been reported for an applied voltage of 9 kV (23:3687). The inherent problem of different focal points for the blue writing beam and the red readout beam will require further research before it can be corrected. Based on the experimental results, there is no doubt that BSO crystals can perform real time lens aberration correction. However, the problems of low diffraction efficiency and different focal points for the two object beams must be solved before the synthetic-aperture optical system depicted in this thesis effort can be of any use to the Air Force.

Recommendations

The foremost area needing further research is creating a common focal point for the different wavelengths of the writing and readout beams. One way to make this problem less severe is to use achromatic lenses for the synthetic aperture. This allows the two different color beams to focus at the same longitudinal point. The drawback is an achromat must be designed for two specific wavelengths and the magnification difference associated with the different colors of incident light can not be corrected. An in-depth study of various electro-optic materials available should be conducted to determine the material best suited for synthetic-aperture aberration correction. Another material which does not require readout at a different wavelength might be available. The best way to eliminate chromatic aberrations is through the use of reflective optics. Eventually, an experimental synthetic-aperture optical system employing reflective optics must be designed and researched in order to prove the use of electro-optic crystals for synthetic-aperture aberration correction.

The low diffraction efficiency was very evident in the synthetic aperture experiment. As previously mentioned, a voltage applied across the crystal would increase the diffraction efficiency significantly. Special care must be taken if the applied voltage is more than 2 kV. Investigation into the equipment and design needed to

supply as much as 8 kV across the crystal should be performed.

Another problem that developed in Experiment 3 was the poor quality of the reference beam. The acquistion of a long focal length (1500 mm), high quality, plano-convex lens would solve this problem. A spatial filter and collimating lens assembly which could be adjusted for different plane wave beam diameters would negate the need for a lens to focus the reference beam. Such equipment needs to be acquired before further synthetic-aperture experiments are conducted.

The final recommendation is to perform a theoretical analysis of exactly where different light rays are focused by a synthetic aperture consisting of reflective optics. The analysis should also include the type equipment and an appropriate design needed to experimentally verify that electro-optic crystals can effectively correct synthetic-aperture aberrations.

Bibliography

1. Amodei, J. J. "Electon Diffusion Effects During Hologram Recording in Crystals," _Applied Physics Letters_, _43_: 22-24 (January 1971).

2. Ashkin, A. and others. "Optically-Induced Refractive Index Inhomegeneities in $LiNbO_3$," _Applied Physics letters_, _9_: 72 (1966).

3. Chen, F. S. and others. "Holographic Storage in Lithium Niobate," _Applied Physics Letters_, _13_: 223-224 (October 1968).

4. Chen, F. S. "Optically Induced Change in Refractive Indices in $LiNbO_3$," _Journal of Applied Physics_, _40_: 3389-3396 (July 1969).

5. Collier, Robert J. and others. _Optical Holography_. New York: Academic Press, 1971.

6. Fienberg, J. D. and others. "Photorefractive Effects and Light-Induced Charge Migration in Barium Titanate," _Journal of Applied Physics_, _51_: 1297-1305 (January 1979).

7. Fisher, Robert A. _Optical Phase Conjugation_. New York: Academic Press, 1983.

8. Gill, Capt Charles W. _Holographic Correction of Aberrations in Optical Systems Employing Synthetic Apertures_. MS Thesis AFIT/GHE/ENP/87-4. School of Engineering, Air Force Institute of Technology (AU), Wright-Patterson AFB OH, March 1987.

9. Glass, A. M. and others. "High-Voltage Bulk Photovoltaic Effect and the Photorefractive Process in $LiNbO_3$," _Applied Physics Letters_, _25_: 233-235 (August 1974).

10. Goodman, Joseph W. _Introduction to Fourier Optics_. San Francisco: McGraw Hill, 1968.

11. -----. "Synthetic Aperture Optics," _Progress in Optics, Vol VIII_, edited by Emil Wolf. LOndon: North Holland Publishing Company, Ltd., 1970.

12. Gunter, P. "Holography, Coherent Light Amplification and Optical Phase Conjugation with Photorefractive Materials," _Physics Reports (Review Section of Physics Letters)_, _93_: 199-299 (January 1982).

13. Hariharan, P. "Holographic Recording Materials: Recent Developments," *Optical Engineering, 19*: 636-641 (October 1980).

14. Hecht, Eugene and Alfred Zajac. *Optics*. Reading PA: Wesley Publishing Company, 1979.

15. Jacobs, Capt David A. *Correcting Aberrated Wavefronts from Synthetic Apertures Holographically*. MS Thesis AFIT/GEP/ENP/86D. School of Engineering, Air Force Institute of Technology (AU), Wright-Patterson AFB OH, December 1986.

16. Johnston, W. D. "Optical Index Damage in $LiNbO_3$ and Other Pyroelectric Insulators," *Journal of Applied Physics, 41*: 3279-3285 (July 1970).

17. Kukhtarev, N. V. "Holographic Storage in Electrooptic Crystals. I. Steady State," *Ferroelectrics, 22*: 949-960 (January 1979).

18. Kuzilin, Yu. E. and V. N. Sintsov. "Holographic Synthesis of a Composit Telescope," *Optical Spectroscopy, 36*: 352-353 (March 1974).

19. Leatherman, Capt Phillip. *Nonlinear Optical Phase Conjugation in Flourescein and Bismuth Silicate (BSO)*. MS Thesis AFIT/GEO/ENP/87D. School of Engineering, Air Force Institute of Technology (AU), Wright-Patterson AFB OH, December 1987.

20. Malacara, Daniel, ed. *Optical Shop Testing*. New York: John Wiley & Sons, 1978.

21. Marciniak, Capt Michael. *Tutorial Presentation of Nonlinear Optical Phase Conjugation with Emphasis on Optical Phase Conjugation in Photorefractive Crystals*. MS Thesis AFIT/GEO/ENP/87D-3. School of Engineering, Air Force Institute of Technology (AU), Wright-Patterson AFB OH, December 1987.

22. Marrakchi, A. and J. P. Huignard. "Diffraction Efficiency and Energy Transfer in Two-Wave Mixing Experiments with $Bi_{12}SiO_{20}$," *Applied Physics, 24*: 131-138 (January 1981).

23. Peltier, M. and F. Micheron. "Volume Hologram Recording and Charge Transfer Process in $Bi_{12}SiO_{20}$ and $Bi_{12}GeO_{20}$," *Journal of Applied Physics, 48*: 3683-3690 (September 1977).

24. Staebler, D. L. and J. J. Amodei. "Coupled-Wave Analysis of Holographioc Storage in LiNbO$_3$," _Journal of Applied Physics_, _43_: 1042-1049 (March 1972).

25. Townsend, R. L. and J. T. LaMacchia. "Optically Induced Refractive Index Changes in BaTiO$_3$," _Journal of Applied Physics_, _41_: 5188-5192 (December 1970).

26. Upatnieks, J. and others. "Correction of Lens Aberrations by Means of Holography," _Applied Physics_, _5_: 589-593 (April 1966).

27. Vahey, David W. "A Nonlinear Coupled-Wave Theory of Holographic Storage in Ferroelectric Materials," _Journal of Applied Physics_, _46_: 3510-3515 (April 1975).

28. Young, L. and others. "Theory of Formation of Phase Holograms in Lithium Niobate," _Applied Physics Letters_, _24_: 264-265 (March 1974).

Vita

Captain David M. Tripp was born on 6 June 1957 in Tullahoma, Tennessee. He graduated from high school in Winchester, Tennessee in 1975. He later attended Motlow State Community College where in 1981 he received an Associates of Science degree in Engineering. He then graduated from Tennesse Technological University in 1983 with a Bachelor of Science degree in Electrical Engineering. Upon graduation from Officer Training School, he was commissioned into the Air Force on 9 September 1983. His first assignment was at the Air Force Space Technology Center, Kirtland AFB where his duties included the management of infrared detector development programs for the Strategic Defense Initiative. He entered the electro-optics graduate program at Air Force Institute of Technology in May 1986.

Permanent address: Route 4 Box 310
                      Tullahoma, Tennessee 37388

REPORT DOCUMENTATION PAGE

1a. REPORT SECURITY CLASSIFICATION	1b. RESTRICTIVE MARKINGS
Unclassified	

2a. SECURITY CLASSIFICATION AUTHORITY	3. DISTRIBUTION/AVAILABILITY OF REPORT
2b. DECLASSIFICATION/DOWNGRADING SCHEDULE	Approved for public release; distribution unlimited.

4. PERFORMING ORGANIZATION REPORT NUMBER(S)	5. MONITORING ORGANIZATION REPORT NUMBER(S)
AFIT/GEO/ENP/87D-5	

6a. NAME OF PERFORMING ORGANIZATION	6b. OFFICE SYMBOL (If applicable)	7a. NAME OF MONITORING ORGANIZATION
School of Engineering	AFIT/ENG	

6c. ADDRESS (City, State and ZIP Code)	7b. ADDRESS (City, State and ZIP Code)
Air Force Institute of Technology Wright-Patterson AFB OH 45433-6583	

8a. NAME OF FUNDING/SPONSORING ORGANIZATION	8b. OFFICE SYMBOL (If applicable)	9. PROCUREMENT INSTRUMENT IDENTIFICATION NUMBER

8c. ADDRESS (City, State and ZIP Code)	10. SOURCE OF FUNDING NOS.			
	PROGRAM ELEMENT NO.	PROJECT NO.	TASK NO.	WORK UNIT NO.

11. TITLE (Include Security Classification)
See Box 19

12. PERSONAL AUTHOR(S)
David M. Tripp, B.S., Capt

13a. TYPE OF REPORT	13b. TIME COVERED		14. DATE OF REPORT (Yr., Mo., Day)	15. PAGE COUNT
MS Thesis	FROM	TO		

16. SUPPLEMENTARY NOTATION

17. COSATI CODES			18. SUBJECT TERMS (Continue on reverse if necessary and identify by block number)
FIELD	GROUP	SUB. GR.	Synthetic Aperture, Aberrations, Correction, photorefractive effect, diffraction grating, bismuth silicon oxide, thesis
20	06		

19. ABSTRACT (Continue on reverse if necessary and identify by block number)

Title: HOLOGRAPHICALLY CORRECTING SYNTHETIC-APERTURE ABERRATIONS

Thesis Advisor: James P. Mills, Lt Col, USAF

Approved for public release: IAW AFR 190-1.

LYNN E. WOLAVER 31 Dec 87
Dean for Research and Professional Development
Air Force Institute of Technology (AFIT)
Wright-Patterson AFB OH 45433

20. DISTRIBUTION/AVAILABILITY OF ABSTRACT	21. ABSTRACT SECURITY CLASSIFICATION
UNCLASSIFIED/UNLIMITED ☒ SAME AS RPT. ☐ DTIC USERS ☐	Unclassified

22a. NAME OF RESPONSIBLE INDIVIDUAL	22b. TELEPHONE NUMBER (Include Area Code)	22c. OFFICE SYMBOL
James P. Mills, Lt Col, USAF	513-255-2012	AFIT/ENP

DD FORM 1473, 83 APR   EDITION OF 1 JAN 73 IS OBSOLETE.

The effectiveness of using a bismuth silicon oxide (BSO)
electro-optic crystal to holographically correct synthetic-
aperture aberrations is investigated. A theoretical analysis
of hologram formation in electro-optic crystals was performed.
Experiments were then conducted to determine the diffraction
efficiency and hologram erasure rate characteristics of the
BSO crystal.   The BSO crystal successfully performed real
time aberration correction of a single-lens optical system;
but due to the experimental synthetic-aperture optical
design, it was impossible for the crystal to correct the
synthetic-aperture aberrations. *Keywords → x- field E*

END

DATE
3-88
DTIC